Young's modulus variation of a variable stiffness element based on jamming of compliant granules

Bachelor's Project - Autumn 2016

Frédéric Freundler, SVBA5 Student, EPFL

Supervisors: Simon Lukas Hauser & Mehmet Mutlu, PhD Students at the BioRob Lab, EPFL

Contents

Abstract

Whether in the scientific or medical field, one requires to work with tools than can switch from a soft, hence adaptive and compliant behaviour to a stiffer one, enhancing precision and controllability. In the surgical field, for instance, an actuator would need to be compliant to its uneven surroundings, capable of adapting to shocks and unequal forces, as well as being stiff enough to perform a rather precise work. In the scope of this bachelor's semester project, which is incorporated within the framework of a climbing robot as well as mimicking soft paw-pads for the Oncilla robot, we created an element offering a wide range of compliance, going from soft (having an elasticity modulus of 0.03 MPa) to stiff (1.9 MPa) while offering a linear spectrum of intermediate behaviours, and then characterised its stiffness along this range, focusing on its Young's elasticity modulus E. In order to achieve that, we designed our element as a membrane containing a granular medium and then stiffened it by vacuuming out the air inside at several pressures (from 1000 mbar to 0 mbar,) with a smartphone controlled device including a pump coupled with a pressure sensor. In the end, we conducted static tests in compression with a professional extensometer and were able to observe a rather linear relation between the internal pressure and the E-modulus for a sample with a quite constant arrangement of the cubes, ensuring a continuous compliance throughout the vacuuming range for a fixed shape. However, the modulus being way inferior to that of the same material in its *concrete* form, future work in this scope would need studying the effect of the stochastic arrangement between the cubes, which seems to play a significant role in the medium's elasticity, as well as trying to conduct the same tests but with a laterally inextensible membrane such as fabric or a metal frame .

1 Introduction

When speaking about variable stiffness elements, one of the many ways to achieve this is using a granular medium. The renowned *universal gripper* [2] has become a classic in this domain. The gripper consists of a membrane (or a *balloon*) stuffed with ground coffee particles which, at atmospheric pressure, adapts to any object and is then hardened by vacuuming out the air inside the membrane, exerting now different forces on the object which allow the gripper to manipulate it (see Fig.1). But such a gripper shows a binary behaviour, since it goes from totally soft when at atmospheric pressure to fully hard-vacuumed without showing a real intermediate state. In addition, the ground coffee which constitutes the medium can be considered as many particles, showing no particular elastic nature and, therefore, no specific compliance. In comparison, the material we chose shows an elastic behaviour, and is capable of compliance.

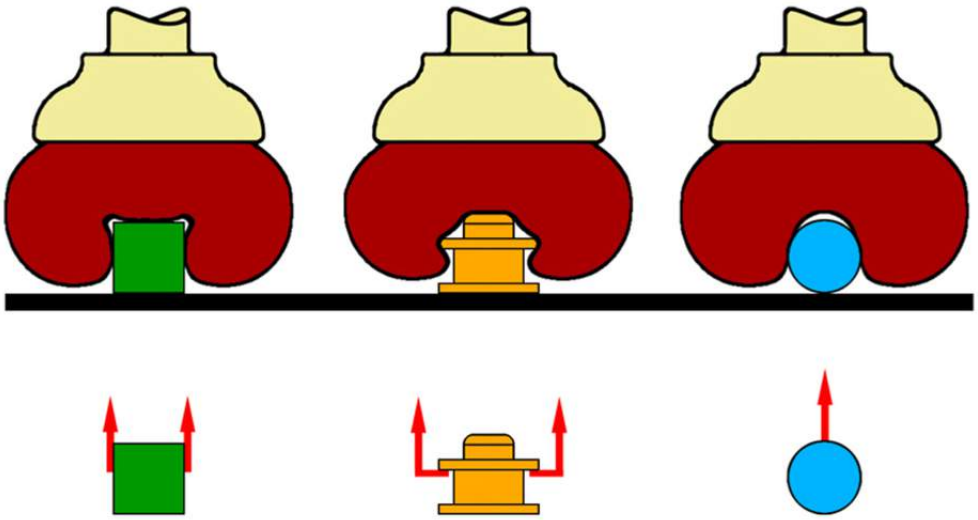

Figure 1: The three types of force that the universal gripper exerts on an object when hardened: LEFT: Static friction form surface contact. CENTER: Geometric constraints from clamping. RIGHT: Vacuum suction. [2].

Based on the previous work done on the subject [5], we chose a polyurethane elastomer of hardness shore 75A (see Fig.2). The chosen shape for the granules was solid 4mm plain rubber cubic granules which, despite having a lower maximum stiffness than other shapes such as spherical beads, shows the least variability and the best linear fashion when undergoing stress at various vacuum pressures.

The material had been tested in *bending* strain [5] [1] but, in the context of the climbing robot, (or mimicking paw-pads for the quadruped robot Oncilla (BioRob)), the main stress we are interested in is *compressive* (see Fig.3). Indeed, to achieve climbing, the robot relies on compliance: whereas *particle* granules such as ground coffee would only adapt to the wall's surfaces, the cube granules, being made of elastic rubber, act like so many little springs exerting a force on the wall, enabling the robot to pull up exactly like a human would. In this scope, the experiment was then focused on retrieving the Young's modulus (compression modulus, commonly abbreviated E) of our granular medium. In the particular Oncilla frame, compliance of the paw-pads is required at the gait level: in slow gait, soft feet are needed, which provide high adaptability to the ground's asperities as well as slow energy exchanges. In rapid gait or running though, the feet would need to be stiffer, in order to show a bouncier behaviour (that is, faster energy exchanges) [3].

To retrieve the compressive elasticity modulus, we had to think about a specific experiment design, and especially on how to put our medium in a standard shape for static

compression measurements and how to actually conduct those experiments. Furthermore, we had a hint that the modulus would vary depending on how packed the granules were: we expected a very low Young's modulus for *loose* granules (that is, at atmospheric pressure) and a high one for a tightly packed medium (at ∼0 mbar internal pressure). Therefore, in order to get a linearly evolving modulus, we would have to measure it at several internal pressures - that is, from atmospheric pressure (*soft*) to quasi-total vacuum (*stiff*). Finally, we made the hypothesis, throughout the whole process, that the material, behaving linearly in bending deflection, would behave likewise in compressive strain.

Figure 2: The two components Neukadur ProtoFlex HS 75A polyurethane elastomer from Altropol used to create the granules.

(a)

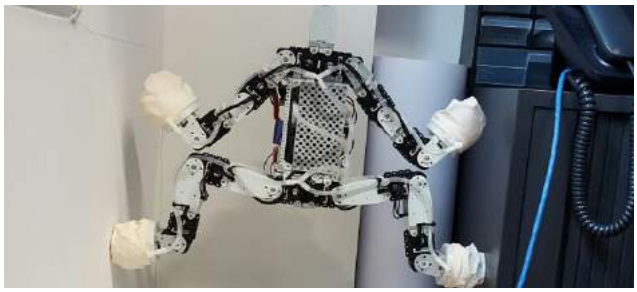

(b)

Figure 3: (a) Zoom on the paw-pads prototypes on the Oncilla robot, when at atmospheric pressure (left) and when vacuumed (right). (b) The Climber, a robot that climbs thanks to the compliance of the medium: it is the elasticity of the granules that allows the climbing by exerting forces on the walls. If the granules would be inelastic (such as for ground coffee), the membrane would only embrace the walls surface's shape without exerting any forces on them: the Climber would fall. In this particular context, we are interested in retrieving the material's modulus in compression.

2 Experiment design

To retrieve the Young's modulus of the material, we had to conduct compressive stress experiment with an extensometer[1] and design an experiment protocol as well as some items.

2.1 Granules

The first step was to create the medium. In order to achieve that, the elastomer was prepared and vacuumed to get rid of potential bubbles which could alter the strength an geometry of the cubes and then poured into a 4 mm by 4 mm by 200 mm mold. After that, the resin was polymerised in an oven at 70 C for 45min. That allowed us to get elastomer strings which were then manually cut in order to obtain 4x4x4 mm cubes. The operation was repeated until the sufficient amount of cubes was reached (see Fig.4).

Figure 4: LEFT: 4x4x4 mm cubes elastomer cubes used as medium. RIGHT: Total amount of cubes retrieved and the scalpel used to cut them.

2.2 Membrane

Once this was done, we had to figure out a way to keep our medium in a standard cylindrical shape throughout the experiments[2] (with $height = 2diameter$). The chosen container for the medium was an oblong latex balloon of nominal dimensions of 20 cm in length, 5cm in diameter and of $\sim$80 µm in thickness. Following the conclusions of previous research done on the subject, latex was indeed the membrane material that shows the best linear characteristics as well as the smallest hysteresis [4]. Note that the actual dimensions of the cylinder, in view of the exact dimensions of the membrane, were 9 cm for the length and 4.5 cm for the diameter.

[1] Instron^{TM}Non-Contacting Advanced Video Extensometer 2, Catalog No. 2663-901.

[2] This standard was communicated by us by the Department of Material Sciences, EPFL

2.3 Hard shell

The medium being granular, the main challenge we encountered was to shape it as desired. Indeed, the membrane being elastic and having a non flat end, it naturally ends up having a shape more like a warhead than a cylinder. In order to frame it as wanted, what we called a *hard shell* was designed[3] (see Fig.5) and 3D printed (see Fig.6).

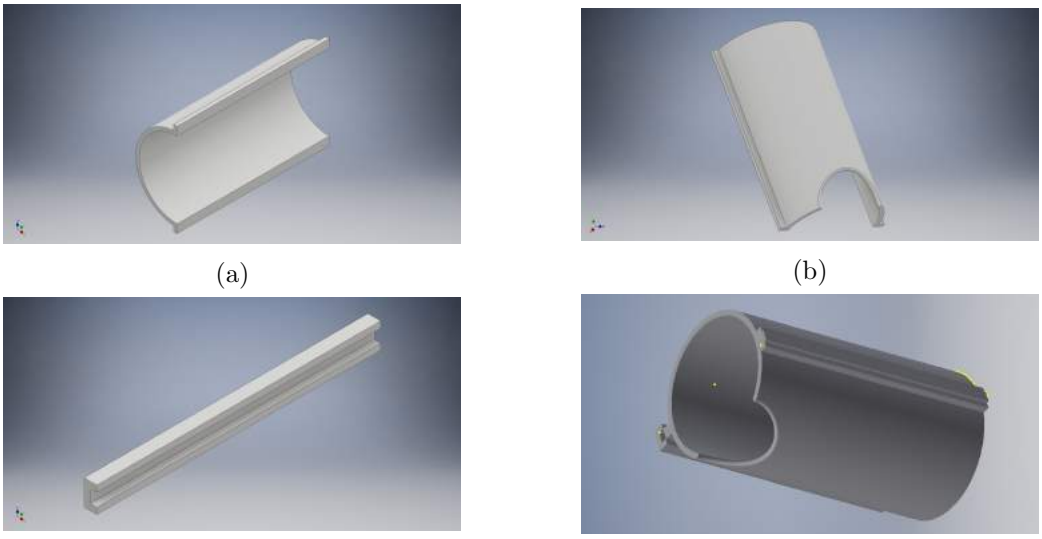

(a) (b) (c) (d)

Figure 5: (a) Half of the side shell: the radius is 2.25 cm, the height is 9 cm and the thickness is 2 mm. (b) Other side, with same dimensions but with a notch in it to allow the inclination of the membrane in order for the base of the membrane to not get in the way of the extensometer's load transmitters at the top and bottom of the cylinder. (c) One of the two so called *holders* that allow us to maintain the shell locked as we vacuum the membrane while shaping it. (d) 3D assembly of every 4 parts composing the shell.

[3] Using the Autodesk Inventor^{TM}CAD software

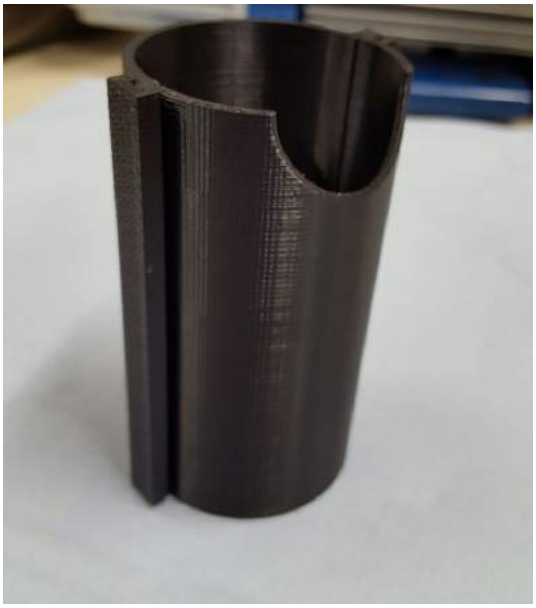

Figure 6: The assembled 3D printed hard shell which was used in the scope of our experiments.

2.4 Variable stiffness element

The design of the element itself is based on the universal gripper [2] and consists in the latex membrane pinched between two hard plastic rings, that form an airtight base. The base is then linked to an airtight switch, enabling us to detach the sample from the vacuuming system to take it into the extensometer (see Fig.7). To avoid the membrane to being sucked in the valve's hole and therefore blocking the air from going out, a small polyurethane tube was glued to the inner side of the base, ensuring that the air outtake is set within the granules (see Fig.8). Note that the pipe is smaller than the cubes, so that they cannot be sucked inside.

Figure 7: The variable stiffness element we designed and used to retrieve our medium's Young's modulus, in its vacuumed state. The membrane has been shaped with the hard shell beforehand. An airtight switch in the *off* state is attached to the base, ensuring the airtightness of the element when removed from the pump. The diameter is 4.5 cm and the length 9 cm.

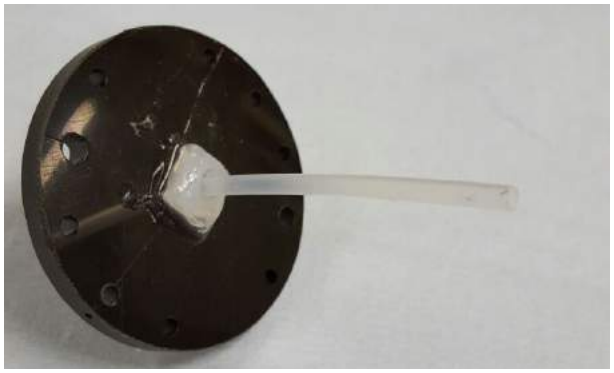

Figure 8: One part of the base (inner side) and the pipe glued to the valve's opening in order to ensure that the membrane is not sucked by the pump, blocking the airflow.

2.5 Electronics

Concerning the electronics used, a setup was designed beforehand. It consists of a Bluetooth smartphone-controlled vacuum system, driven by a DAQ card (Arduino). A vacuum pump is plugged in the base of the element and sucks the air out of the membrane. In order to do tests at discrete pressures, a pressure sensor is included in the airflow circuit that sends information about the inner pressure to the computer. The pump was linked to the membrane via a T-valve, in order for the airflow to go from the membrane to the pump and to pass through the pressure sensor. A similar test setup can be seen in Fig.9.

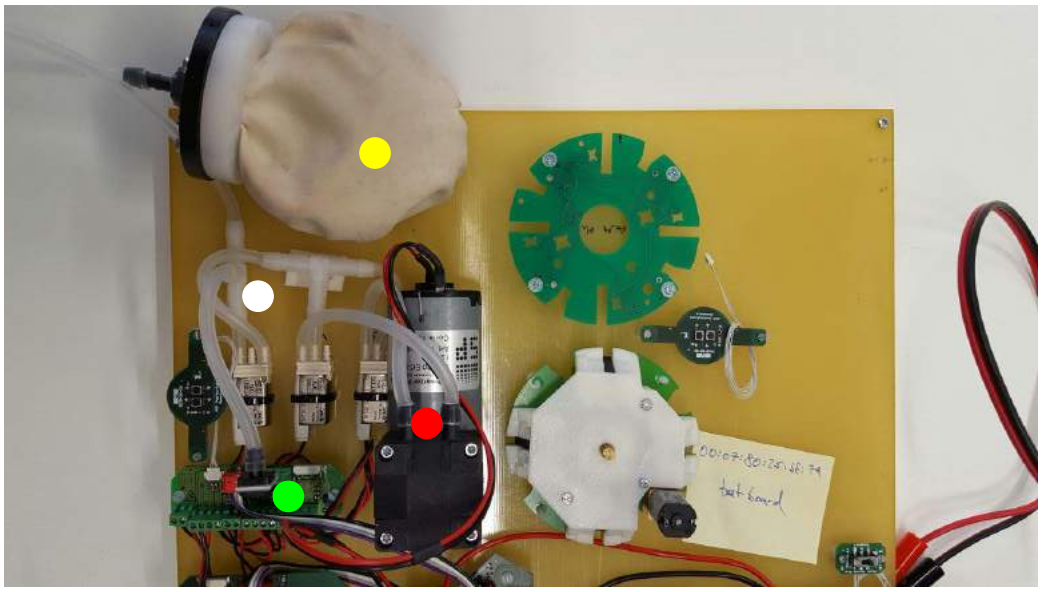

Vacuuming Test Setup

Test element composed of a latex balloon filled with cubes, and a base;

T-valve allowing the airflow going from the membrane to be sensed by the pressure sensor

Vacuum Pump

Pressure Sensor

Figure 9: A test setup similar to the one used for our experiments. The cables are linked to the DAQ system. However, this setup is not controlled by bluetooth.

We needed then to create the extensometer experimental protocol itself:

1. At first, we needed to shape the membrane using the hard shell: the air was sucked out from the membrane until the pressure sensor sensed that the inner pressure had reached the desired value, with a ± 5 mbar imprecision due to the pump (see Fig.10);
2. After that, the hard shell was removed from the pump drain and in order for the specimen to be taken to the extensometer without inflating back, the airtight switch valve was set to the *off* state (see Fig.7).
3. The sample was then put into the extensometer to perform the compressive tests (see Fig.11).

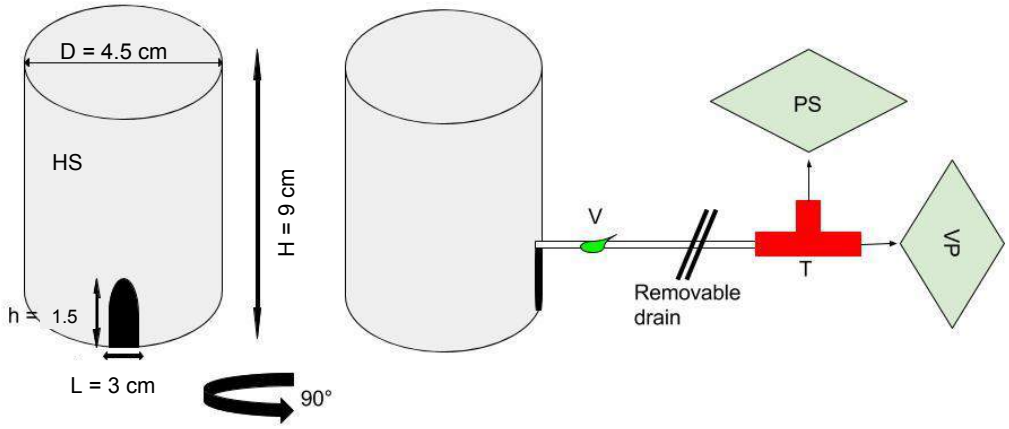

Legend:

HS: Hard Shell used to mold the element.
V: Switch valve ensuring that the vacuum is maintained when we remove the drain from the pump setup.
PS: Pressure Sensor
VP: Vacuum Pump
T: T-valve that allow the airflow created by the pump to reached the PS in order to measure the pressure.

Figure 10: Scheme of the shaping process right before taking the sample to the extensometer.

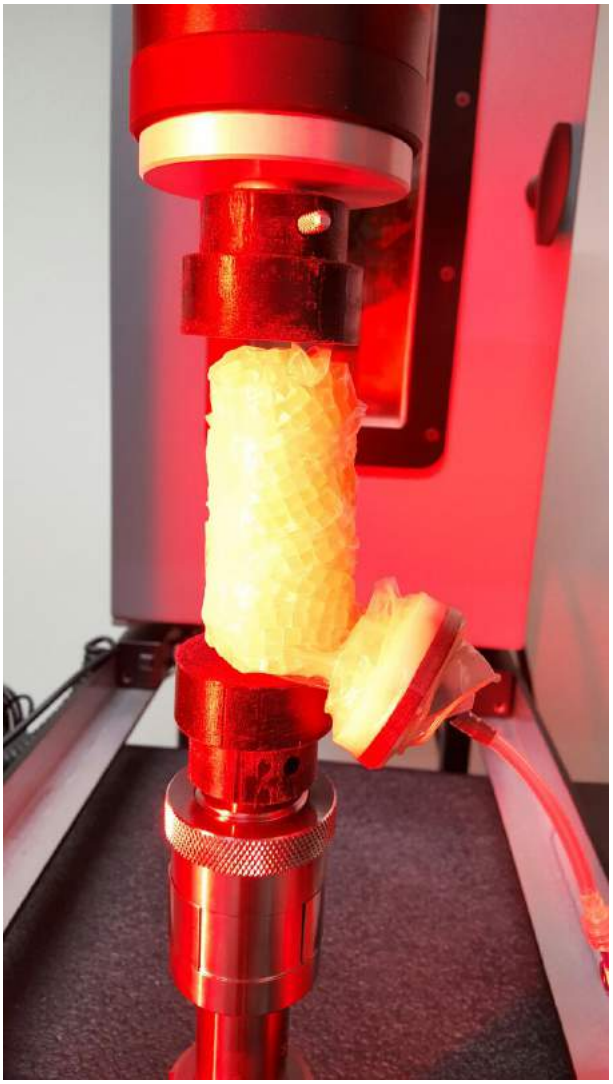

Figure 11: A view of the element (*specimen*) between the force transmitters of the extensometer. The red light comes from the extensometer's video module and enhances the contrast in order to further evaluate the lateral expansion of the specimen (NB: we did not use this feature for our experiments). One can easily see that the base is tilted to the side in order for it not to get in the way of the load transmitters.

4. The test itself, a static compressive test with fixed maximum displacement, consisted of the following steps:

   (a) At a speed of 20 mm/min, a load was applied by the machine on the top of the sample, progressively compressing it;
   (b) When the fixed value of 3 mm vertical displacement was reached, the loading process ended;
   (c) Right after that, the sample was let free to expanse back to its original shape while pushing up the load transmitter;
   (d) When the load transmitter was subject to a null force, the program ended and raw data (Load/Displacement) was retrieved.

   For each pressure, 5 tests were conducted on the sample, in order to have more representative results and to ensure reproducibility. The element was inflated back and then vacuumed between each compression for a given pressure, but it was hardly reshaped, and so the cubes were scarcely rearranged.

5. We also conducted, for each pressure, a test to see the creep of the cubes - that is, their rearrangement when subjected to stress. The test protocol was:

   (a) At a speed of 20 mm/min, a load was applied by the machine on the top of the sample, progressively compressing it;
   (b) When the fixed value of 3 mm vertical displacement was reached, the loading process ended;
   (c) The system held this position for 60 seconds;
   (d) Right after that, the sample was let free to expanse back to its original shape while pushing up the load transmitter;
   (e) When the load transmitter was subject to a null force, the program ended and raw data (Load/Displacement) was retrieved.

   For the creep, we conducted only one test for each pressure, because we lacked the time and did not want to characterise the creep so much as merely stating its existence.

Finally, a Matlab^{TM}script was implemented, that calculated the E-modulus for every trial following the equation 1

$$E = \frac{\sigma}{\epsilon} = \frac{F/A_o}{\Delta L/L_o} = \frac{FL_o}{\Delta L A_o} \tag{1}$$

(where F is the maximum load when the displacement is maximal at ΔL (3 mm), L_o is the original length of 9 cm and A_o is the area on which the load is applied, which is

equal to 63.61 cm^2 and is calculated with πR^2 with $R = 2.25$ cm) and the mean value of the modulus between the trials for each pressure, as well as the mean standard deviation between each pressure's trials. The program in the end gave up a curve for the modulus as a function of the membrane pressure. We also calculated an order 1 linear approximation for the curve in the scope of verifying the hypothesis that the modulus behaves linearly with respect to the inner pressure. For the creep, we simply retrieved graphs of the force over displacement as well as force as a function of time.

3 Results and Discussion

The Instron^{TM}program yielded three data: time, load and compressive displacement. From that, we plotted several graphs exhibiting the following results:

3.1 Force Measurements

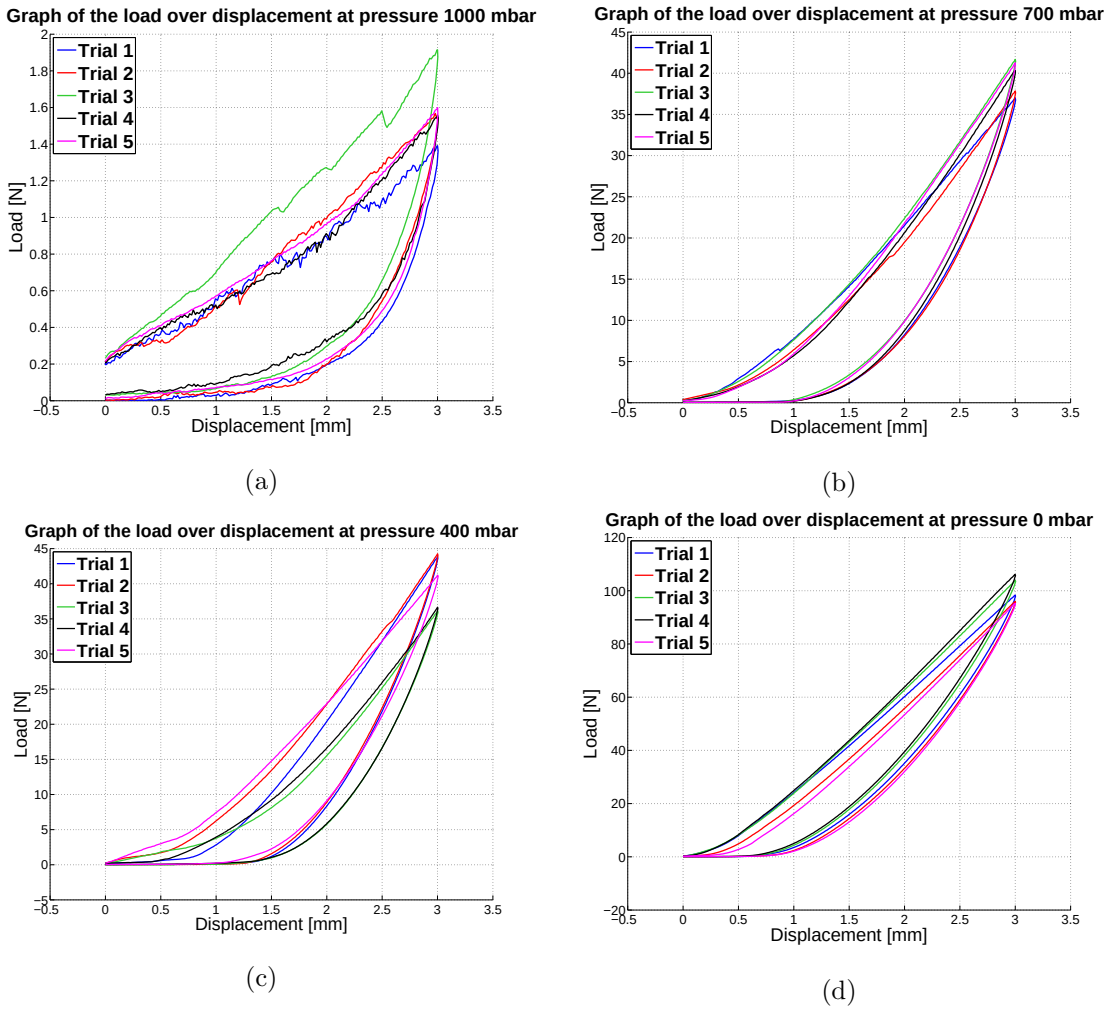

Figure 12: Load over displacement curves from the experiment (without measuring the creep) for (a) atmospheric pressure, (b) 700 mbar, (c) 400 mbar, (d) 0 mbar (vacuum). Note that the pressures were reached with a ± 5 mbar precision.

As you can see in the four examples in Fig.12, we first plotted the hysteresis curves for each pressure (the rest of the plots are shown in appendix A). The hysteresis is hard to quantify for the atmospheric pressure sample, since the medium is quite loose and the cubes are hardly contained by the latex membrane. It is however easily noticeable and quantifiable as soon as low vacuum is applied. We were able to notice that with lower pressures, the hysteresis seems to diminish. Indeed, the sample loses between 1 and 1.5 mm irrespective to its original height for pressures above 300 mbar and decreases to around 0.75 mm or less for inferior pressures. However this decrease is not linear: it is rather constantly around 1 to 1.5 mm for a 900-300 mbar and then drops suddenly below one and stays quite constant for a 300-0 mbar range. Additionally, the more the pressure approaches vacuum, the more the hysteresis curve tends to linearize and sharpen. These phenomena are due to the cubes being packed more tightly with lower inner pressures, resulting in the granular medium mimicking the behaviour of the full material more and more, but reaching a modulus more than thrice lesser than that of the full material.

3.2 E-Modulus

Compiling each mean E modulus (stress/strain) as well as the standard deviation for each pressure gave the curve in Fig.13, which has a correlation coefficient with respect to a linear regression of 0.95271. Note that for 100% vacuum, the E-modulus is ∼1.9 MPa, whereas the modulus of the full material (i.e. the resin in its concrete form) is of 6.5 MPa, calculated using the following formula [6]

$$shore\_\mathrm{erf}\_75 = 100 * \mathrm{erf}(3.186 \cdot 10^{-4} \sqrt{(E \cdot 10^6)}.$$

, where $shore\_\mathrm{erf}\_75$ is the 75A hardness shore of the material and E the modulus to be determined.

The cubes can be seen as so many tiny springs, being stacked in series and parallel in a container. Would the cubes be perfectly stacked on top of each other in our cylindrical membrane, we would retrieve the same modulus as for the full material by addition of every spring stiffness coefficient k. However, the cubes' jamming implies that the cubes can either stack with their sides along a horizontal line (that is, parallel to the ground) or diagonally, in a stochastic process and the spring stiffness along the diagonal of a cube is not the same as between two sides. Moreover, the elastic membrane hardly contains the lateral expansion of our cylindrical sample. The addition of these two phenomena brings the value of our Young's modulus to a lesser number than for the concrete material. Despite this difference due to the very nature of the granular medium and its stochastic jamming as well as taking into account the nature of the membrane, the E modulus as a function of the inner pressure (Fig.13) can be approximated in a linear way, with a correlation coefficient of 0.95271. Note that this linear behaviour was measured for an approximately similar arrangement of the cubes throughout the experiment. We observed indeed rather significant modulus fluctuations for a same pressure when the medium was firmly shaken

before reshaping, so we tried to handle it carefully, in order not to mix the cubes too much. Additionally, the sample had to be loaded perfectly perpendicular, otherwise some sort of sliding would have occured.

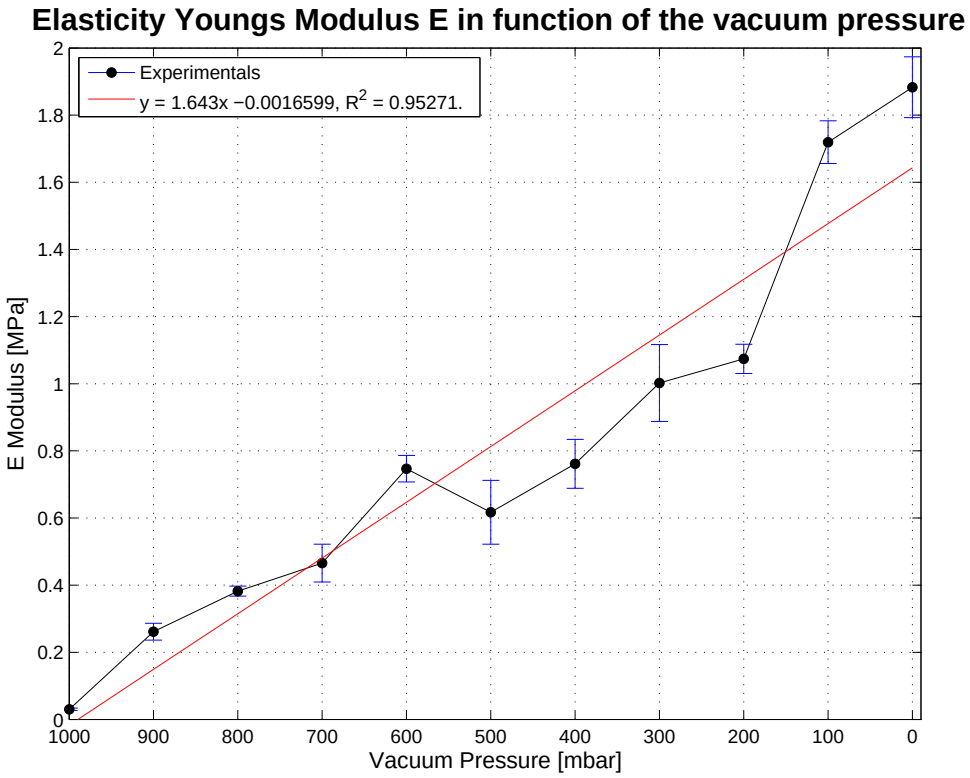

Figure 13: E-Modulus in function of the membrane's inner pressure, with the standard deviation for each pressure as well as a linear regression of the data and the correlation coefficient.

3.3 Creep

Finally, with the creep experiment, we were able to retrieve the graphs displayed in Fig.14 and appendix B, showing the cubes' rearrangement on each other within a 60 second time span for the each pressure.

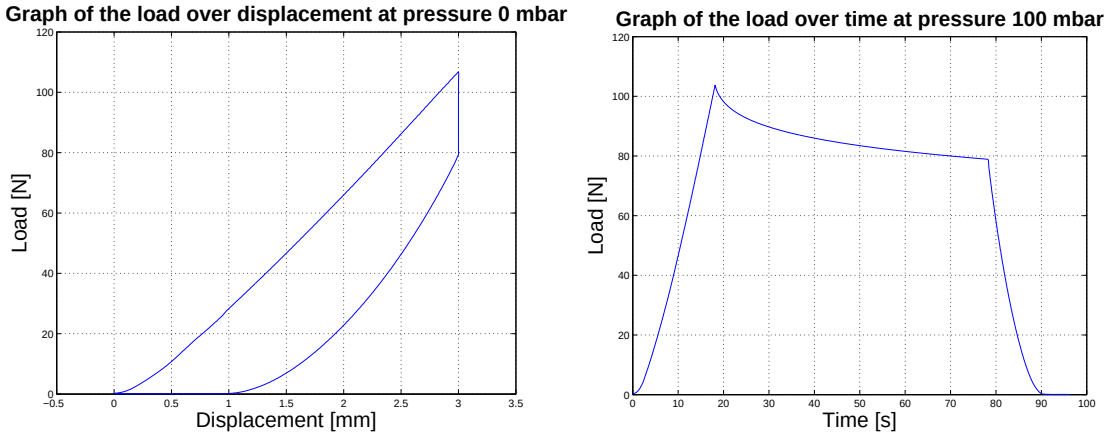

Figure 14: Display of the creep at 0 mbar. LEFT: Graph of the load/displacement ratio, where the creep is displayed by the vertical segment at 3 mm displacement: the displacement is maintained and the cubes rearrange, resulting in a load drop. RIGHT: view of the same creep displayed as load in function of time. Right after compression stops, the load decays rapidly at first and then tends to converge with time.

Regarding the creep, an identical behaviour was observed throughout the pressure range, with a more marked stabilisation for the lowest pressure, due to the cubes being more tightly packed with the increasing vacuum. As displayed in the right graph on Fig.14, after the compression stops, when the hold begins (at around 18 seconds), the cubes rearrange rapidly, due to the load exerting a consequent force "jolt" at this point (i.e. the $\frac{dF}{dt}$ derivative is almost vertical). The jolt decreases with time and after 5 seconds, it is already twice lesser than at the beginning. Indeed, because of the cubes rearrangement and collapsing, the load on the sample decreases (as seen on the left graph of the figure) and the cubes, subjected to a lesser and lesser force, will eventually stop creeping, which is displayed on the right graph, with the curve flattening with time. After the hold stops, the sample is free to expand again. As described above, we used an elastic membrane, mainly due to the fact that in the scope of application we are interested in, we need such an elastic membrane, which can adapt to uneven terrain. Using a rigid membrane, such as textile, is expected to impair the creep by constraining the cubes within an inextensible frame.

4 Conclusion and Future Work

Regarding the stiffness variability of the element, we stated the hypothesis that it would behave in a linear manner in compression, such as it responded to bending stress. According to the results we obtain, the Young's modulus E can be approximated as a linear function of the inner pressure with a correlation coefficient of 0.95271. Therefore, the variable stiffness element is indeed able to exhibit a continuous compliance within a pressure range going from atmospheric to vacuum. However, such a behaviour was measured for a quasi similar cubes' arrangement and we have seen that another arrangement for the same pressure could impair the modulus and that we only reached less than a third of the full material's modulus. Hence, even if the modulus is a material property and is the same for both full material and the cubes, the E we obtained, which depends only on pressure in our model, should in fact be considered as non constant, by mean of a lack of understanding the arrangement process, and be modeled as depending on both the pressure *and* the stochastic jamming of the cubes.

Future works on understanding or anticipating the stochastic arrangement probability of the cubes might help modeling the Young's modulus as a two variable function. In this scope, assessing the level of dependance between the pressure and the arrangement would probably be needed. As for the creep, we have seen that it somehow seems to converge at some point. Using a more rigid membrane would diminish it, but in the framework of the climber and the Oncilla, we need an elastic membrane which can adapt to an irregular terrain, so possible works to come on the subject would have to focus on increasing the thickness of the membrane, which could prevent the expansion without impairing its adaptability. With the creep phenomenon, the load decreases with time, implying a less important grip on an object or surface. When speaking about gait, this is not significant since the contact between the variable stiffness element and the surface would only last as long as it takes for the robot to achieve one step. Concerning the climber though, it would be interesting to measure the time before the force exerted by the robot's feet on the walls is not sufficient enough to prevent it from falling down. Should the element be used to grip and move objects for a significant time, similar experiments should be conducted.

Finally, the time needed to pump the air out of the membrane implies a delay, which can slow the robots movements, implying that the pump is the limiting factor in many cases. Since speed is often required in the medical scope for instance, future work on the vacuuming delay would be useful.

5 Acknowledgements

I wish to epxress my grateful thanks to Simon Hauser, who took the time to provide me with the necessary knowledge and help in order to accomplish this work.

A Plots of the load over displacement for every pressure

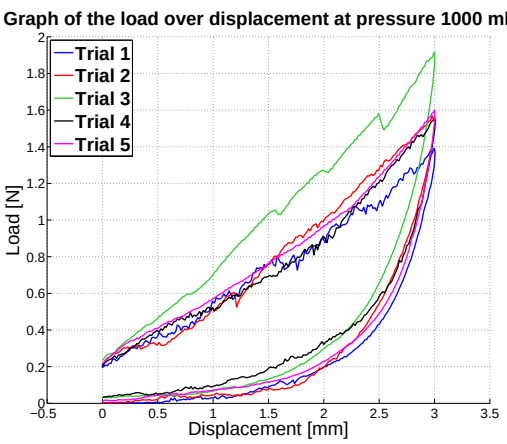

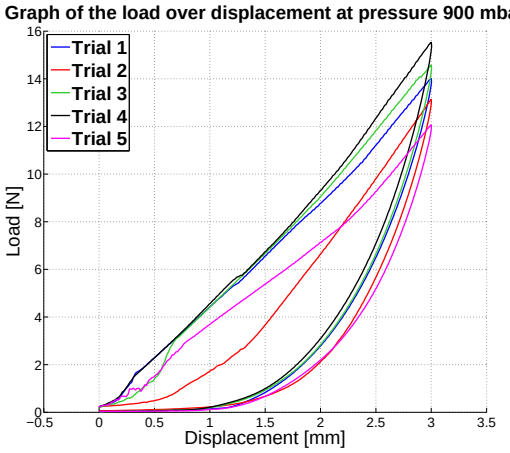

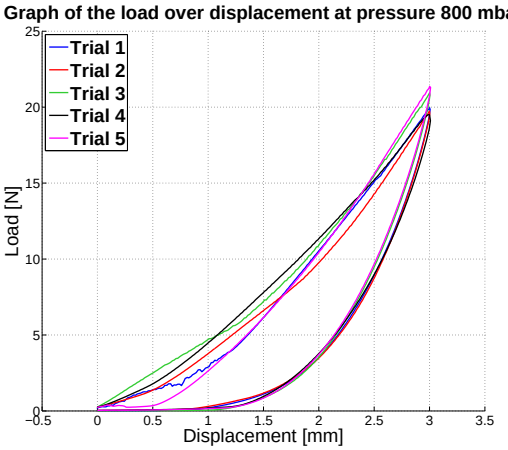

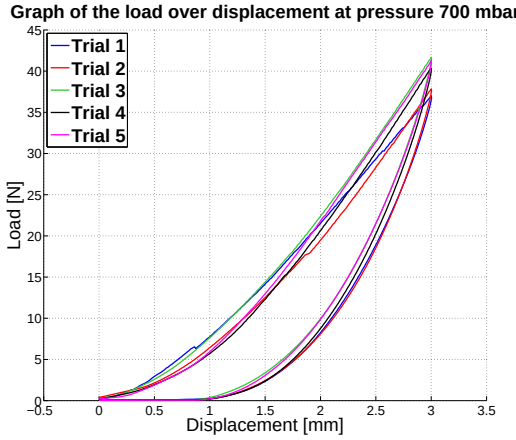

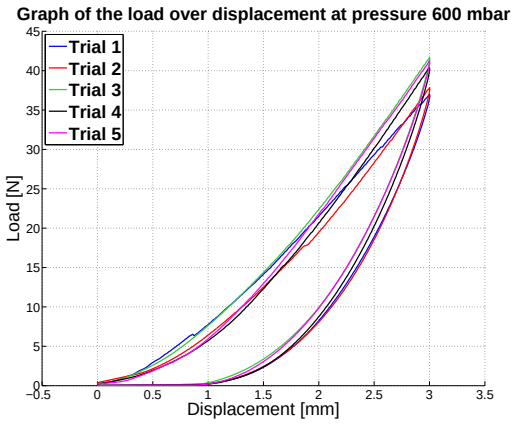

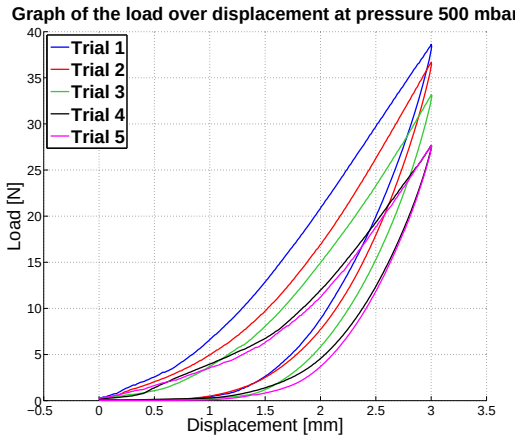

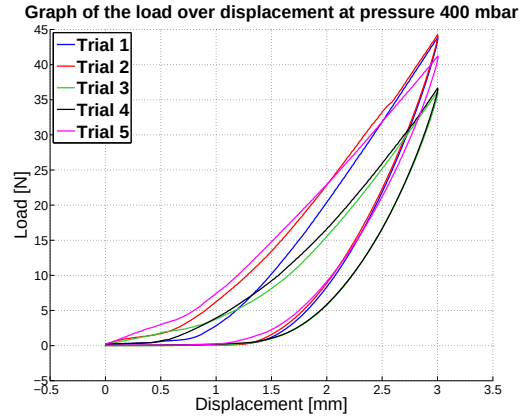
Graph of the load over displacement at pressure 400 mbar
Trial 1
Trial 2
Trial 3
Trial 4
Trial 5
Load [N]
Displacement [mm]

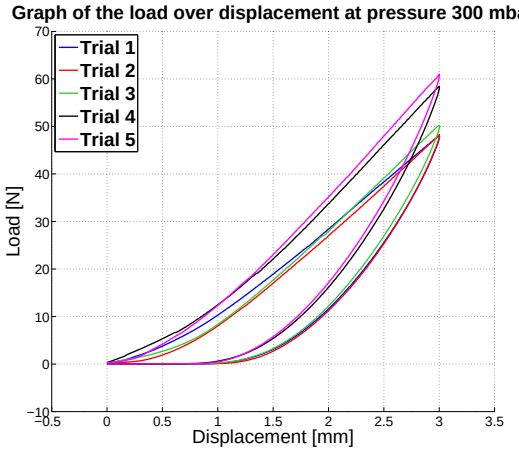
Graph of the load over displacement at pressure 300 mbar
Trial 1
Trial 2
Trial 3
Trial 4
Trial 5
Load [N]
Displacement [mm]

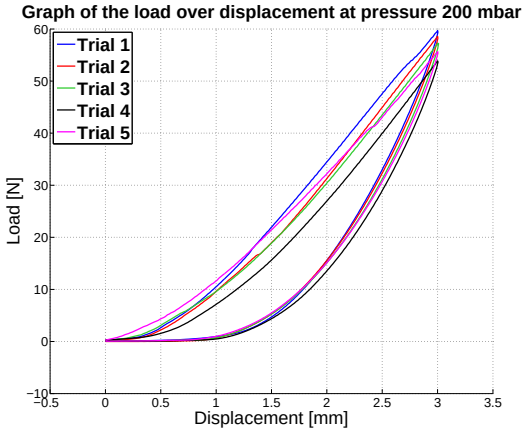
Graph of the load over displacement at pressure 200 mbar
Trial 1
Trial 2
Trial 3
Trial 4
Trial 5
Load [N]
Displacement [mm]

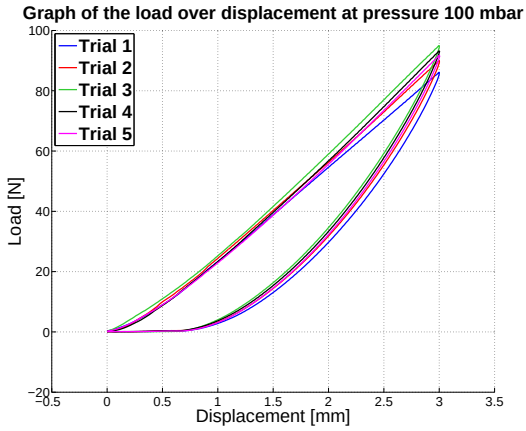
Graph of the load over displacement at pressure 100 mbar
Trial 1
Trial 2
Trial 3
Trial 4
Trial 5
Load [N]
Displacement [mm]

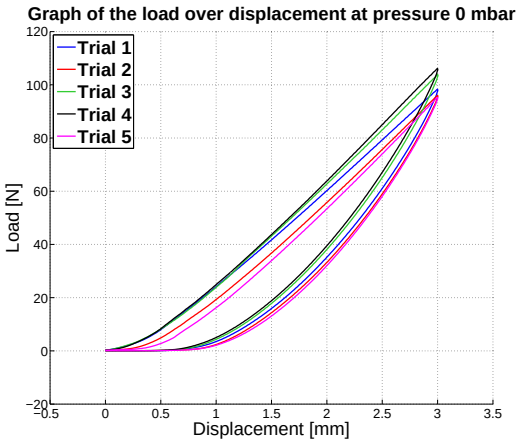
Graph of the load over displacement at pressure 0 mbar
Trial 1
Trial 2
Trial 3
Trial 4
Trial 5
Load [N]
Displacement [mm]

B Creep: plots of the load as a function of displacement and time

Graph of the load over displacement at pressure 1000 mba

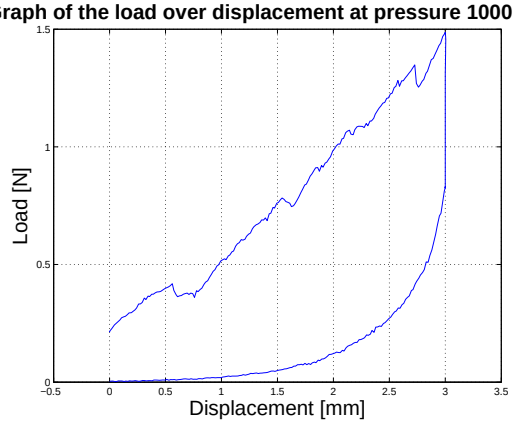

Graph of the load over time at pressure 1000 mbar

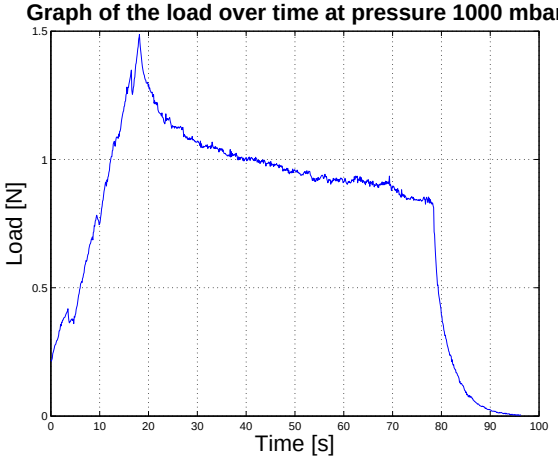

Graph of the load over displacement at pressure 900 mba

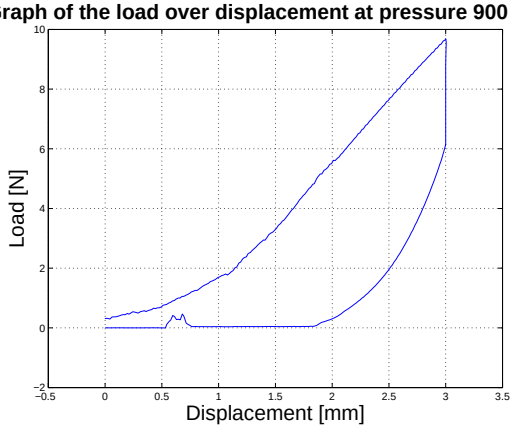

Graph of the load over time at pressure 900 mbar

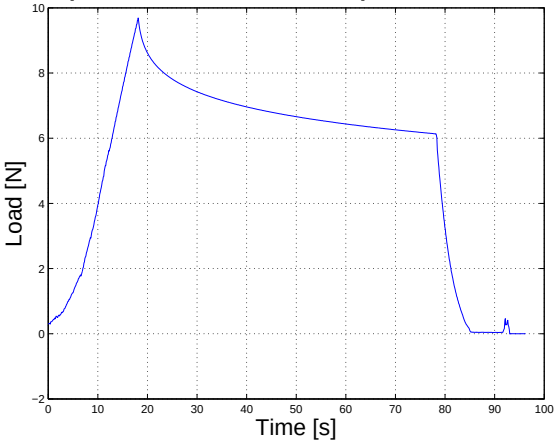

Graph of the load over displacement at pressure 800 mba

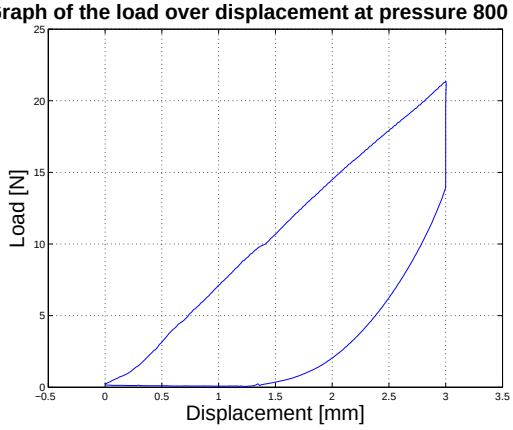

Graph of the load over time at pressure 800 mbar

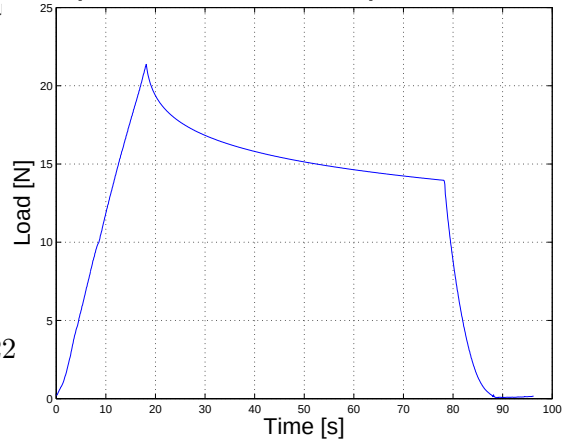

Graph of the load over displacement at pressure 700 mba

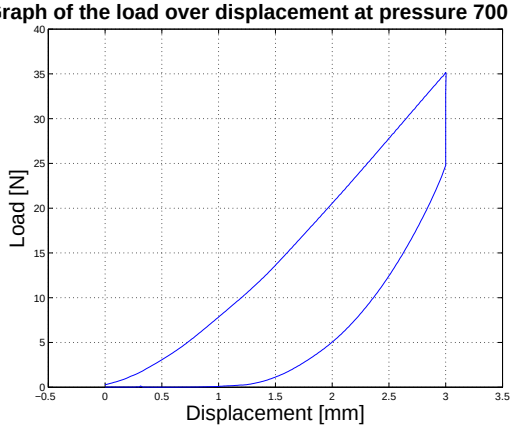

Graph of the load over time at pressure 700 mbar

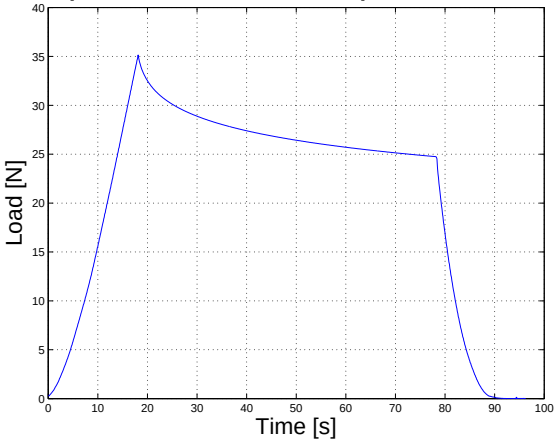

Graph of the load over displacement at pressure 600 mba

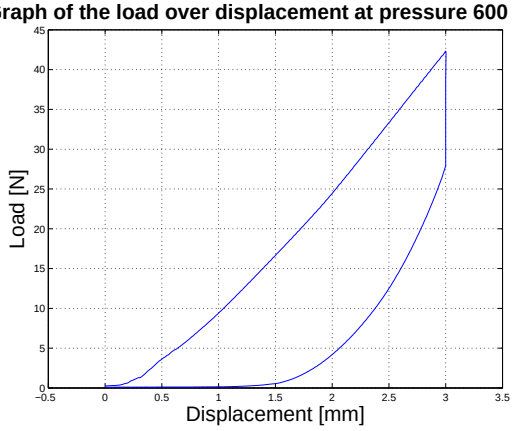

Graph of the load over time at pressure 600 mbar

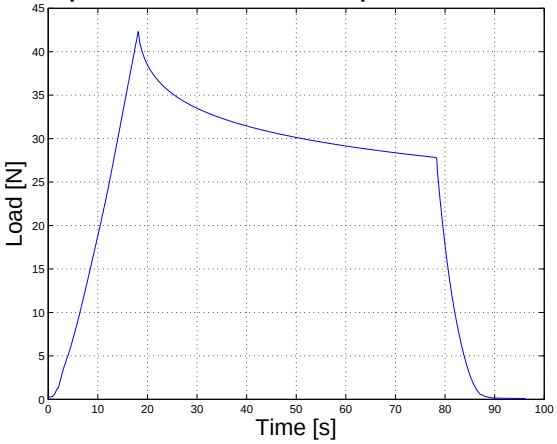

Graph of the load over displacement at pressure 500 mba

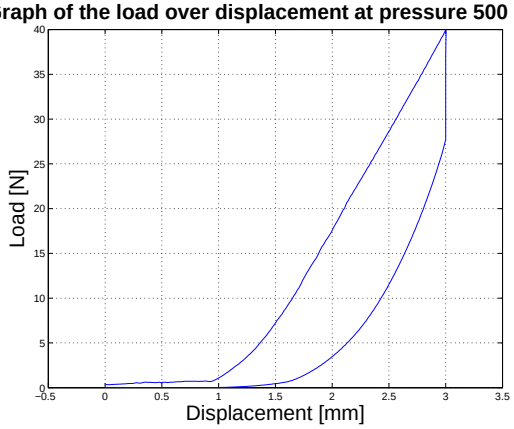

Graph of the load over time at pressure 500 mbar

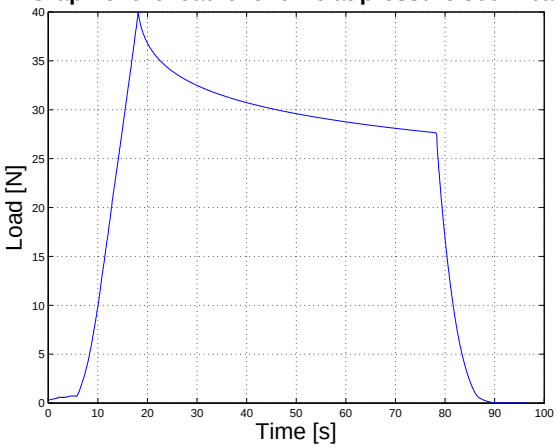

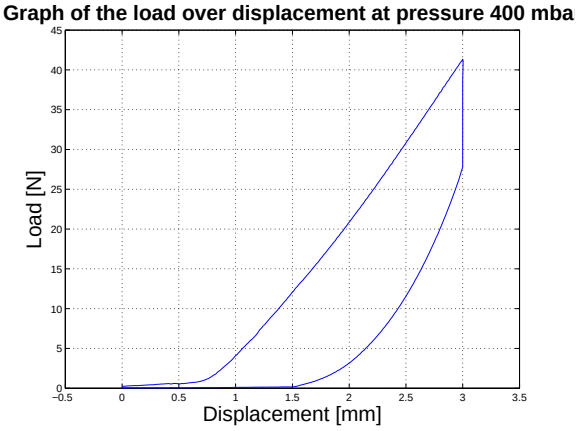
Graph of the load over displacement at pressure 400 mba
Load [N]
Displacement [mm]

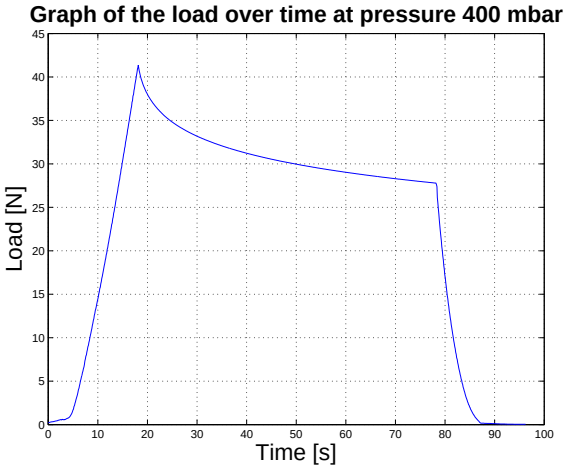
Graph of the load over time at pressure 400 mbar
Load [N]
Time [s]

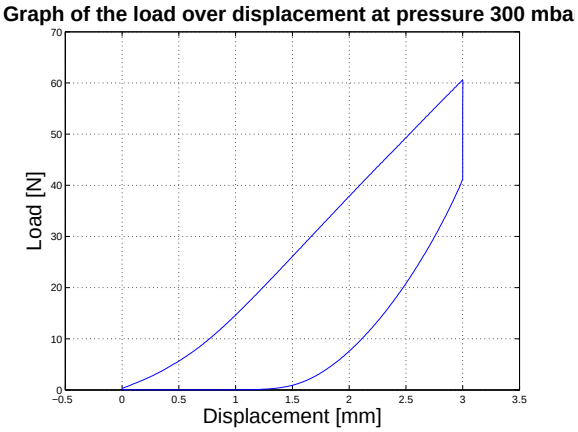
Graph of the load over displacement at pressure 300 mba
Load [N]
Displacement [mm]

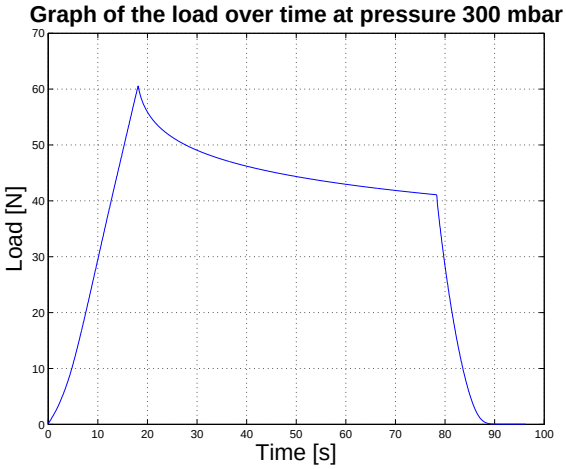
Graph of the load over time at pressure 300 mbar
Load [N]
Time [s]

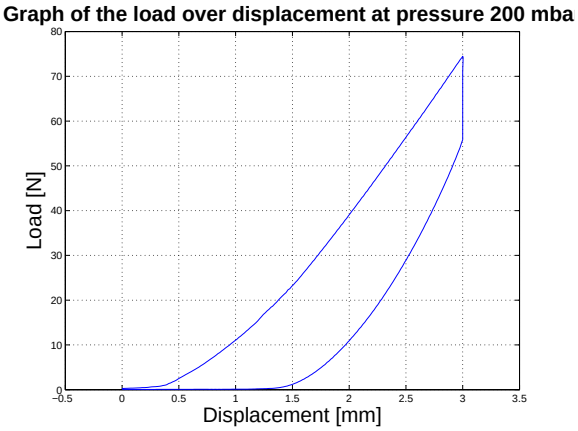
Graph of the load over displacement at pressure 200 mba
Load [N]
Displacement [mm]

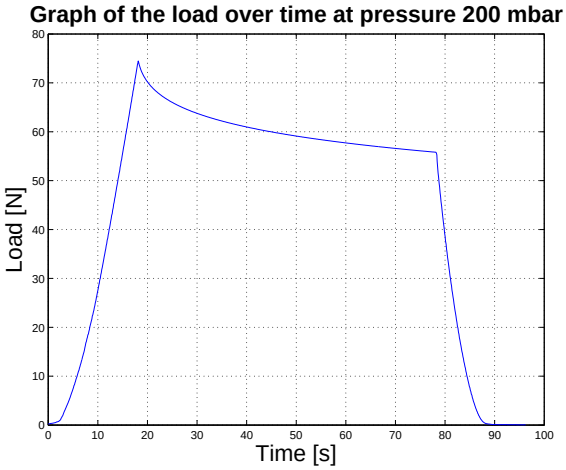
Graph of the load over time at pressure 200 mbar
Load [N]
Time [s]

Graph of the load over displacement at pressure 100 mba

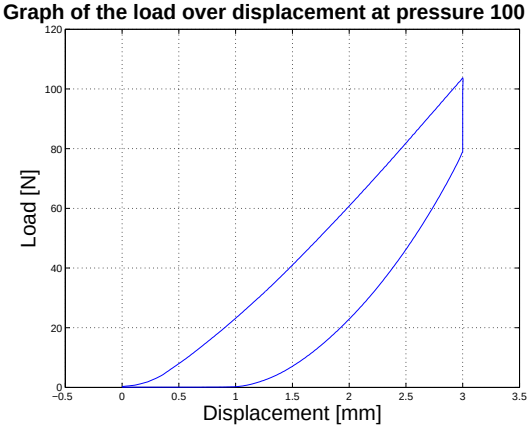

Graph of the load over time at pressure 100 mbar

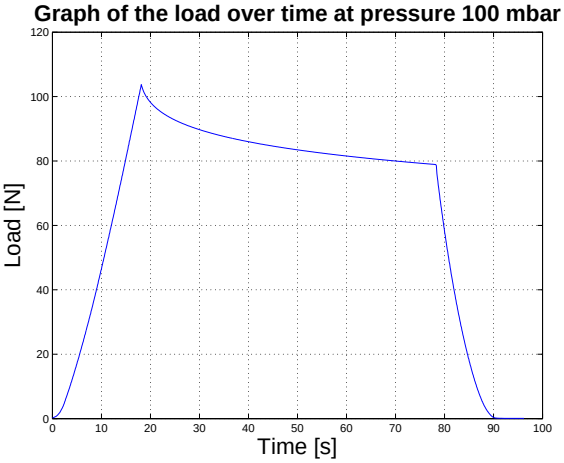

Graph of the load over displacement at pressure 0 mbar

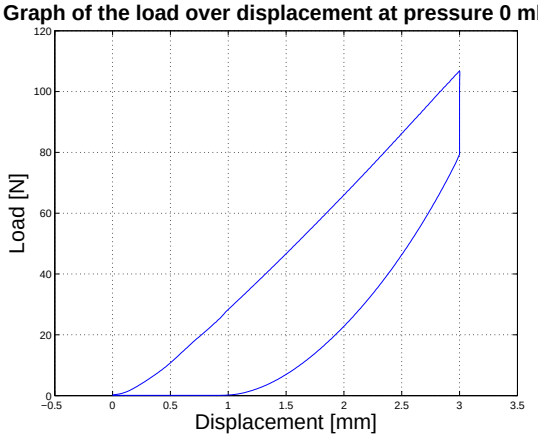

Graph of the load over time at pressure 100 mbar

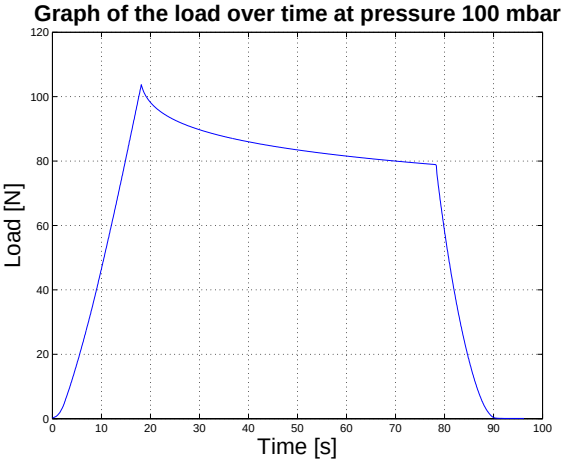

References

[1] Jiang Allen, Ashgar Ataollahi, Kaspar Althoefer, Prokar Dasgupta, and Thrishantha Nanayakkara. "A variable stiffness joins by granular jamming". *Proceedings of the ASME 2012 International Design Engineering Technical Conferences And Computers and Information in Engineering Conference IDETC/CIE 2012*, August 2012.

[2] John R. Amend Jr., Eric Brown, Nicholas Rodenberg, Heinrich M. Jaeger, and Hod Lipson. "A positive pressure universal gripper based on the jamming of granular material". *IEEE Transaction On Robotics*, 28(2), April 2012.

[3] Simon Hauser, Peter Eckert, Alexandre Tuleu, and Auke Ijspeert. "Friction and damping of a compliant foot based on granular jamming for legged robots"riction and damping of a compliant foot based on granular jamming for legged robots". *6th IEEE RAS/EMBS International Conference on Biomedical Robotics and Biomechatronics (BioRob)*, June 2016.

[4] Allen Jiang, Tommaso Ranzani, Giada Gerboni, Laura Lekstutyte, Kaspar Althoefer, Prokar Dasgupta, and Thrishantha Nanayakkara. "Robotic granular jamming: Does the membrane matter?".

[5] Allen Jiang, Georgios Xynogalas, Prokar Dasgupta, Kaspar Alhoefer, and Thrishantha Nanayakkara. "Design of a variable stiffness flexible manipulator with composite granular jamming and membrane coupling". *IEEE/RSJ International Conference on Intelligent Robots and Systems, Vilamoura, Algarve, Portugal*, October 2012.

[6] Irani M. Methathananda, Sandra Parker, Mangala P. Patel, and Michael Braden. "The relationship between shore hardness of elastomeric dental materials and young's modulus". *Dental Materials*, 25(8):956–959, August 2009.